Supplementary information on geochronology

Age models were based on downcore radionuclide activities (^{241}Am, ^{210}Pb), as well as on six calibrated radiocarbon ages each for both the Callao and the Pisco cores. For Callao, the model was constrained by relating slumps with information of large historic marine earthquakes that had rupture zones near the core site (Dorbath et al., 1990).

The presence in the core tops of protruding filaments of the giant sulphur bacteria *Thioploca* spp., which lives in the sediment water interface, confirmed that the sediment surface was recovered in both box cores. The cores lost humidity and shrank during the time period elapsed between coring and sub-sampling, leaving free space to the liners. Thus it was necessary to apply a correction for the sedimentation area and the dry bulk density. We measured the core width and length at discreet depths, and then fit the relationship between the core area and the core depth by minimum squares. Since the core shrinkage diminished with core depth until the core area fit exactly into the liner, it was possible to calculate the percent area loss at each core sediment depth or at each sample layer. We used this factor to correct the volume of each sample layer and then to correct the dry bulk density (DBD) and the mass flux ($g_{\text{dry weight}}$ cm^{-2}). DBD estimates varied two fold above the lithological shift, and four-fold throughout downcore (Figure 3a, j). Since an assumption of constant density cannot be made, we employed the accumulated mass instead of sediment depth for fitting the age models in order to avoid compaction artifacts.

The age-mass models were developed removing stratigraphic anomalies believed to be instantaneous deposits. There was one slump near the bottom of the Pisco core while the Callao core had two nearly contiguous slumps in the mid-section and another one near the bottom.

Dating of latest records

Downcore profiles of the bomb-derived ^{241}Am was used to date the uppermost layer of both cores as bomb-derived radionuclides reflect fallout due to atomic bomb testing in both hemispheres since 1953 (Appleby, 2000; UNSCEAR, 2000; Ribeiro & Arribére, 2002) (Table S1). Below the appearance of ^{241}Am in the sediments, excess ^{210}Pb activities were used to fit sedimentation accumulation models until

values reached the ^{210}Pb time-domain, which is considered to be equivalent to six half-lives of ^{210}Pb before present, approximately 135 years ago (Figure S1). While the downcore distribution of excess ^{210}Pb followed an exponential distribution in the Callao core, the downcore distribution in the Pisco core exhibited greater scattering. Therefore a constant flux, constant supply CFCS sedimentation model was applied to the Callao core whereas a constant rate supply CRS sedimentation model (that assumes varying sedimentation rate) was applied to the Pisco core (Appleby, 2000).

Radiocarbon ages of organic matter

Radiocarbon ages of bulk organic matter were used to date the lower section of the cores. The radiocarbon ages increased with accumulated mass but with some scatter, particularly in the case of the Pisco core. Old radiocarbon ages leading to age inversions due to anomalously higher local reservoir age or changing organic matter source were not used in the age model construction (Table S2). For elucidating the origin of organic matter, sediment samples were examined under the petrographic microscope (transmitted light), after separation from carbonate-bearing and silicate phases using acid digestion (palynofacies analysis). This approach leads to the identification of the different organic components and provides a quantitative estimation of their relative abundance (Boussafir et al., 1995).

The downcore profiles of the organic fraction (Palynofacies) and total organic carbon against conventional radiocarbon ages and δ^{13}C of the dated samples revealed the existence of two groups with different organic matter characteristics (Figure S2). The first group dominates the cores and is associated with high content of marine homogenous or granular amorphous organic matter, a signature that is associated with high productivity linked to upwelling (Boussafir et al., 1995; Pichevin et al., 2004; Valdés et al., 2004). This first group was found mostly throughout the Callao core. Two inversions towards older radiocarbon age were identified within this group, which occurred at the lithological shift in the Callao core and at 56 cm depth (Figure S2a) and were interpreted as an amplification of the local reservoir age due to water mass change or stronger upwelling. With the exception of these points, all other data of this group were used for the age model development up to the ^{210}Pb-domain.

The second group of organic carbon characteristics appeared below the lithological shift, particularly in the Pisco core. This group was characterized by anomalously old radiocarbon ages

leading to age inversions, increased content of dispersed amorphous organic matter or slightly increased content of terrestrial plants matter, and very negative values of $\delta^{13}C$ (< -22.5 ‰). Taken together these signatures indicate the contribution of allochtonous, reworked, or even terrestrial organic matter (Meyers, 1997), explaining the older than expected radiocarbon ages (Figure S2b). Therefore, radiocarbon values from this group were not taken into account for the age model development.

Reservoir age calculations and calibration of radiocarbon ages

The radiocarbon age associated with the shift in the Pisco core was aligned with the four radiocarbon ages in the upper part of the core (within the ^{210}Pb-time domain). To calibrate this data point, we first estimated the local reservoir ages (ΔR) for the ^{210}Pb-time domain, which were simply estimated by difference between the ^{210}Pb-derived dates and the conventional ages, minus the global reservoir effect (R) using the marine calibration curve (Hughen et al., 2004). The values were quite similar before 1950 AD, giving an average ΔR of 293 ± 26 y. Therefore we used this ΔR to calibrate the conventional radiocarbon age for the shift.

The average ΔR for the record before the ^{210}Pb-time domain was estimated by applying a linear regression fit to the downcore radiocarbon ages versus the accumulated mass up to the oldest ^{210}Pb-dating point, which had an accumulated mass set to zero. The marine calibration curve (Hughen et al., 2004) was used to determine the average marine reservoir age for the period. The average ΔR was taken as the difference between the regression curve intercept and the average marine reservoir age plus the ^{210}Pb-derived age (Figure S3). Our ΔR estimations with this procedure were 188 ± 79 years for Pisco and 279 ± 53 years for Callao. The values are similar to previous ΔR estimations, based on radiocarbon measurements on marine shells. For Callao, ΔR estimations from four shells collected in 1908 and 1926 AD average 187 ± 51 years (Jones et al., 2007). For the Central Peruvian coast (08 – 14°S), the ΔR is 217 ± 133 years if all the shells used for ΔR estimation are taken into account (Taylor & Berger, 1967; Jones et al., 2007). However, these average values should be taken with caution, due to intrashell variation in radiocarbon age, which can be significant (~200 y) (Jones et al., 2007). In addition, it is possible that radiocarbon ages from the sedimentary organic matter mainly reflect the export production associated with upwelling, leading ΔR towards high values within its whole range.

Estimation of mass accumulation rates and final age models

The average ΔRs before the ^{210}Pb domain for each core were used to determine the calibrated radiocarbon ages in this period of overlap with the software CALIB v. 5.0 (Stuiver & Reimer, 1993; Stuiver et al., 2005). After the calibration, the average mass accumulation rate (MAR) before the ^{210}Pb time-domain was obtained by linear regression of the calibrated radiocarbon ages (means) and the oldest age of the ^{210}Pb time-domain versus the accumulated mass (Table S2).

For the Callao core, the average MAR before the ^{210}Pb-time domain is 0.0174 ± 0.0012 g cm^{-2} y^{-1} (n=7, R^2= 0.98), yielding an age of the record of approximately 720 years. If only the core section between the second and third slump is used, the computed MAR is similar (0.0177 ± 0.0032 g cm^{-2} y^{-1}; n=4, R^2=0.92), and the intercept at the second slump position is 1660 ± 43 AD. Applying either of the two rates, the two upper slumps are dated about 47 years apart. The two largest historic (> 1500 AD) marine earthquakes that hit Callao occurred within 59 years, at 1746 AD (8.6 Mw) and at 1687 AD (8.4 Mw). The other large historic marine earthquake (> 7 Mw) that occurred before 1860 AD was at 1586 AD (8.1 Mw) (Dorbath et al., 1990). Thus, taking into consideration the average MAR, we consider that the two contiguous slumps very likely correspond to the seismic events at 1746 AD and 1687 AD, with some sediment loss, and we used the earthquake dates as time-markers for the age model (Table S1). Note that the chronology adjustment based on the correlations with historical earthquakes is about ten years.

The average MAR mentioned above is significantly lower than the ^{210}Pb-CFCS MAR (0.0306 ± 0.0030 g cm^{-2} y^{-1}, n=6). Thin-section observations across the lithological shift indicate that it is not an unconformity, but a continuous rapid change from one sedimentological unit to another. Therefore,a change in mass accumulation rate across the shift is expected. Applying the average MAR computed before the 1746-slump time marker the shift was dated at 1818 ± 6 AD. In turn, the MAR for the time period between 1860 AD and the date of the sedimentological shift could be estimated as 0.0207 ± 0.0046 g cm^{-2} y^{-1} (Figure 2a).

For the Pisco core, the average MAR before the ^{210}Pb-time domain is 0.0218 ± 0.0013 g cm^{-2} y^{-1} (n=7, R^2= 0.92), yielding an age of the record of approximately 702 years. The rate was significantly lower than the mean ^{210}Pb-CRS MAR, computed for the period between ca. 1935 AD and 1860 AD,

when variation in sediment accumulation was low (0.0297 ± 0.0067 g cm^{-2} y^{-1}, n = 14). Using the average MAR, the lithological shift is dated at 1812 ± 7 AD, which is older than the date based on the ^{210}Pb-CRS model, but within statistical range (1825 ± 9 AD). Here also thin-section observations indicate a shift between different sedimentological units with no unconformity. Although dating resolution here is not sufficient to directly resolve changes in sedimentation across the lithological shift, we estimated the shift date as the mean value from the two estimated dates (1819 ± 12 AD). The sedimentation rate for the time period between 1860 AD and the shift date was then estimated (0.0251 ± 0.0063 g cm^{-2} y^{-1}) as done in the Callao core (Figure 2b).

In summary, the final age model for both cores included: 1) the ^{241}Am/^{210}Pb-derived MAR models from the oldest ^{210}Pb derived-dated point to the present; 2) the intermediate MAR between the shift date and the oldest ^{210}Pb derived-dated point; and 3) the average MAR, based on calibrated ^{14}C ages, for the whole period until the sedimentological shift (Table S2). Time-resolution of the chronologies vary from +/- 1 year in the uppermost part of the cores to +/- 30 years at the bottom (Figure 2).

Supplementary references

Appleby, P.G.: Chronostratigraphic techniques in recent sediments, in: Developments in Paleoenvironmental Research. Volume 1, Tracking Environmental Changes in Lake Sediments: Physical and Chemical Techniques,. Last W.M. & Smol J.P. (Eds.), Kluwer, Dordrecht, The Netherlands, 171-203, 2000.

Boussafir, M., Gelin, F., Lallier-Vergès, E., Derenne, S., Bertrand, P. and Largeau, C.: Electron microscopy and pyrolysis of kerogens from Kimmeridge Clay Formation, UK: source organisms, preservation processes and origin of microcycles, Geochim. Cosmochim. Acta, 59, 3731–3747, 1995.

Dorbath, L., Cisternas, A. and Dorbath, C.: Assessment of the size of large and great historical earthquakes in Peru, Bull. Seismol. Soc. Amer., 80, 551-576, 1990.

Hughen, K. A., Baillie, M. G.L., Bard, E., Beck, J. W., Bertrand, C. J.H., Blackwell, P. G., Buck, C. E., Burr, G. S., Cutler, K. B., Damon, P. E., Edwards, R. L., Fairbanks, R.G., Friedrich, M., Guilderson, T. P., Kromer, B., McCormac, G., Manning, S., Bronk Ramsey, C., Reimer, P. J., Reimer, R. W., Remmele, S.; Southon, J. R., Stuiver, M., Talamo, S., Taylor, F.W., Plicht, J. V. D., Weyhenmeyer, C.E.: Marine04 Marine Radiocarbon Age Calibration, 0-26 Cal kyr BP, Radiocarbon, 46, 1059-1086, 2004.

Jones, K., Hodgins, G., Dettman, D., Andrus, F., Nelson, A. and Etayo-Cadavid, M.: Seasonal variations in Peruvian marine reservoir age from pre-bomb Argopecten purpuratus shell carbonate, Radiocarbon, 49, 877-888, 2007.

Meyers, P.A.: Organic geochemical proxies of paleoceanographic, paleolimnologic, and paleoclimatic processes, Org. Geochem., 27, 213–250, 1997.

Pichevin, L., Bertrand, P., Boussafir, M. and Disnar, J.-R.: Organic matter accumulation and preservation controls in a deep sea modern environment: an example from Namibia slope sediments, Org. Geochem., 35, 543–559, 2004.

Ribeiro Guevara, S. and Arribére, M.: ^{137}Cs dating of lake cores from the Nahuel Huapi National Park, Patagonia, Argentina: Historical records and profile measurements, J. Rad. Nucl. Chem., 252, 37–45, 2002.

Taylor, R. E and Berger, R:. Radiocarbon content of marine shells from the Pacific coasts of Central and South America. Science, 158,1180-1182, 1967.

Stuiver, M., and Reimer, P. J.: Extended ^{14}C database and revised CALIB radiocarbon calibration program, Radiocarbon, 35, 215-230, 1993.

Stuiver, M., Reimer, P. J., and Reimer, R. W. CALIB 5.0. WWW program and documentation. Available at: http://calib.qub.ac.uk/calib/ (2005)

United Nations Scientific Committee on the Effects of Atomic Radiation UNSCEAR. Report to the General Assembly, with scientific annexes.Vol. I, Sources and effects of ionizing radiation. Annex C. Exposures to the public from man-made radiations. 134 p. Vienna, 2000.

Valdés, J., Sifeddine, A., Lallier-Verges, E. and Ortlieb, L.: Petrographic and geochemical study of organic matter in surficial laminated sediments from an upwelling system (Mejillones del Sur Bay, Northern Chile). Org. Geochem., 35, 881-894, 2004.

Supplementary Figure 1

Downcore profiles of excess ^{210}Pb and ^{241}Am in the Callao boxcore B0413 (a) and in the Pisco boxcore B0406 (b). c) reconstructed fallout of ^{137}Cs in the Southern Hemisphere (UNSCEAR, 2000), and fallout specific activity of ^{137}Cs in Buenos Aires (Ribeiro & Arribére, 2002). The prominent features of fallout change (onset and peak periods, shaded) were used to identify three time-markers in the downcore ^{241}Am specific activity for both cores. Time intervals for each time-marker were estimated from excess ^{210}Pb – derived sedimentation rate in the uppermost layer and sample layer thickness.

Supplementary Figure 2

X-ray digital radiographies and downcore profiles of total organic carbon content (%), palynofacies analysis of the organic matter, conventional radiocarbon ages and δ^{13}C of the radiocarbon samples in the Callao boxcore (a) and in the Pisco boxcore (b). The dotted lines highlight old radiocarbon ages leading to significant age inversions (yellow circles) in relation with organic matter properties (see supplementary text on methods). Radiocarbon ages in white circles correspond to the ^{210}Pb-time domain and were not used in the model. Radiocarbon ages in black circles were used for the age models. Amplifications of the three slumps in the Callao core (S1, S2 and S3) and of the slump in the Pico core are showed at left and dotted. The gaps in the ordinate axes of the downcore profiles indicate the slumps' positions.

Supplementary Figure 3

Estimation of the local reservoir age (ΔR) before the late nineteenth century (core B0406, Pisco) was done with a linear regression between conventional ^{14}C age and accumulated mass before the ^{210}Pb time domain. This regression yields the approximate age before present (BP) of the record, for which the average ocean reservoir age (R) is calculated, using the marine calibration curve (Hughen et al., 2004). The difference between the curve intercept and the age BP of the origin (90 ± 5 BP, according to the ^{210}Pb CRS model) is the total reservoir effect (ΔR + R). Thus ΔR is the difference between the total reservoir effect and the average ocean reservoir age (ΔR = 188 ± 79 years). The same procedure applied to the Callao box core yielded a ΔR value equal to 279 ± 53 years.

Supplementary Table S1. Chronology tie-points in the Peruvian margin boxcores, based on age at bottom of sediment samples (see supplementary text). Sediment depths and accumulated masses in brackets correspond to slump bottoms.

Boxcore	sediment depth (cm)			age AD				acc. mass	
	top		bottom	date top		date base	error (y)	(g cm^{-2})	comments
B0413	4.7	-	5.1	1973	-	1970	1	0.75	^{241}Am peak, South Pacific tests (France)
	7.0	-	8.1	1966	-	1962	1	1.28	^{241}Am main peak, Southern Hemisphere (SH) peak of atomic assays
	10.7	-	10.9	1954	-	1952	1	1.77	^{241}Am presence, onset of atomic tests
	25.1	-	25.7	1874	-	1870	10	4.35	^{210}Pb CFCS model (ca. 6 half lifes)
	36.0	-	36.8 (37.2)	1762	-	1746.8	3	6.67 (6.80)	Major earthquake at 1746.8 AD, top (base) of slump
	39.0	-	39.9 (47.3)	1704	-	1687.8	3	7.46 (9.69)	Major earthquake at 1687.8 AD, top (base) of slump
B0406	4.7	-	5.5	1974	-	1970	1	0.88	^{241}Am peak,South Pacific tests (France)
	6.9	-	8.2	1966	-	1962	1	1.27	^{241}Am main peak, SH peak of atomic assays
	11.8	-	12.4	1954	-	1952	1	1.90	^{241}Am presence, onset of atomic tests
	27.3	-	28.4	1867	-	1860	5	4.77	^{210}Pb CRS model (ca. 6 half lifes)

Table S2. Conventional radiocarbon ages, local reservoir ages (ΔR) and calibrated radiocarbon ages from the boxcores off Callao (B0413) and Pisco (B0406). For the latest records ΔRs can be estimated by comparison with the ^{210}Pb-derived ages. Radiocarbon age inversions correspond to change in organic matter source or increased ΔR and were not included for the age model development (Figure 2). Estimation of ΔR before the ^{210}Pb|domain is explained in the text and in Figure 3. All ages are given in years BP.

core	sample code	sed. depth cm	mass. depth g cm^{-2}	^{14}C age (means ± 1S) years BP			ΔR (means ± 1S) years			cal. ^{14}C age (means ± 1S) years BP			age from ^{210}Pb dating years BP			Comments
B01413	B0413-12	11.9	1.954	1155	±	45	686	±	51				2	±	2	ΔR inferred from ^{210}Pb dating
(Callao)	B0413-18	17.5	2.918	805	±	30	390	±	38				33	±	6	ΔR inferred from ^{210}Pb dating
	B0413-22	22.0	3.692	830	±	30	425	±	39				59	±	8	ΔR inferred from ^{210}Pb dating
	B0413-25	25.7	4.347	690	±	45	292	±	52				80	±	10	ΔR inferred from ^{210}Pb dating. Oldest age of ^{210}Pb domain
	B0413-37	33.1	5.426	820	±	45	279	±	53	176	±	86				
	B0413-38	33.7	5.592	1060	±	30										older ΔR
	B0413-42	37.2	6.796	1080	±	50										slump S1, removed
	B0413-43	39.0	7.310	925	±	20	279	±	53	321	±	86				
	B0413-45	40.7	7.832	1075	±	45										slump S2, removed
	B0413-47	42.9	8.368	1140	±	45										slump S2, removed
	B0413-50	47.3	9.692	1160	±	45										slump S2, removed
	B0413-54	51.9	11.117	1000	±	50	279	±	53	363	±	68				
	B0413-59	56.1	12.368	1360	±	60										older ΔR
	B0413-64	60.0	13.544	1180	±	45	279	±	53	511	±	56				
	B0413-68	63.0	14.452	1295	±	45	279	±	53	592	±	52				
	B0413-70	65.8	15.223	1260	±	60	279	±	53	573	±	57				
	B0413-71a	66.7	15.472	1385	±	30										slump S3, removed
	B0413-72a	71.4	16.391	1200	±	30										slump S3, removed
	B0413-74	78.5	17.951	1400	±	45										old OM source
B0406	B0406-16	13.00	1.989	680	±	45	211	±	51				0	±	3	ΔR inferred from ^{210}Pb dating
(Pisco)	B0406-24	18.30	2.919	740	±	30	294	±	38				30	±	4	ΔR inferred from ^{210}Pb dating
	B0406-32	24.80	4.097	760	±	30	292	±	38				67	±	4	ΔR inferred from ^{210}Pb dating
	B0406-35	28.40	4.775	770	±	50	292	±	55				90	±	5	ΔR inferred from ^{210}Pb dating. Oldest age of ^{210}Pb domain
	B0406-40	32.95	5.622	840	±	30	293	±	26	175	±	95				ΔR inferred from upper ^{210}Pb dating (n=3, see text)
	B0406-44	36.25	6.685	700	±	40	188	±	79	150	±	92				
	B0406-49	39.70	7.950	1155	±	30					±					old OM source
	B0406-55	45.05	9.749	1095	±	30					±					old OM source
	B0406-59	48.20	10.635	1145	±	30					±					old OM source
	B0406-66	52.05	11.772	1060	±	45	188	±	79	489	±	78				
	B0406-68	57.30	13.265	1040	±	45	188	±	79	468	±	83				
	B0406-73	60.25	14.326	1315	±	30					±					old OM source
	B0406-78	67.35	16.307	1200	±	30					±					old OM source
	B0406-80	70.20	17.625	1125	±	30	188	±	79	552	±	64				
	B0406-82	71.90	18.264	1215	±	45	188	±	79	596	±	67				

SF1

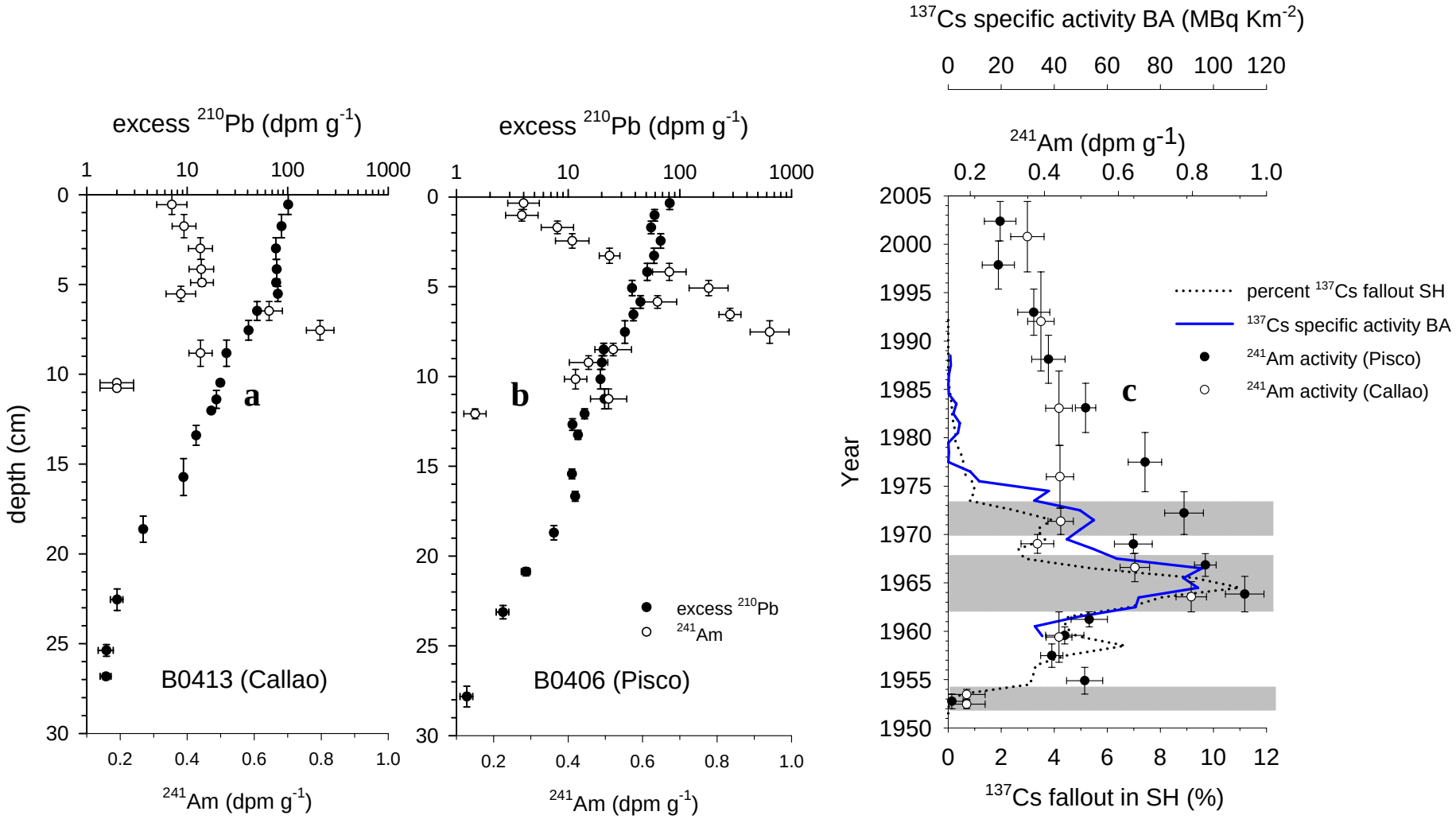
excess 210Pb (dpm g-1)
depth (cm)
a
B0413 (Callao)
241Am (dpm g-1)
b
B0406 (Pisco)
excess 210Pb
241Am
137Cs specific activity BA (MBq Km-2)
241Am (dpm g-1)
Year
c
percent 137Cs fallout SH
137Cs specific activity BA
241Am activity (Pisco)
241Am activity (Callao)
137Cs fallout in SH (%)

SF2

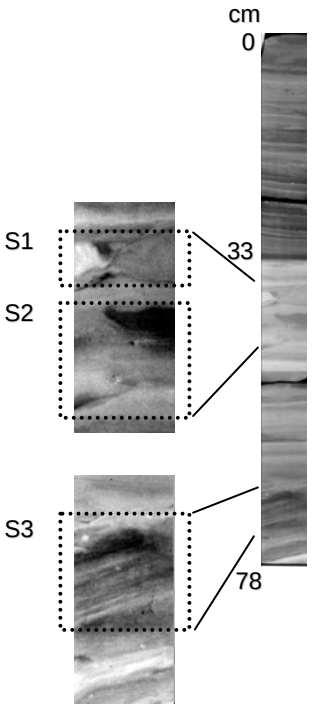
cm
0
S1
S2
S3
33
78

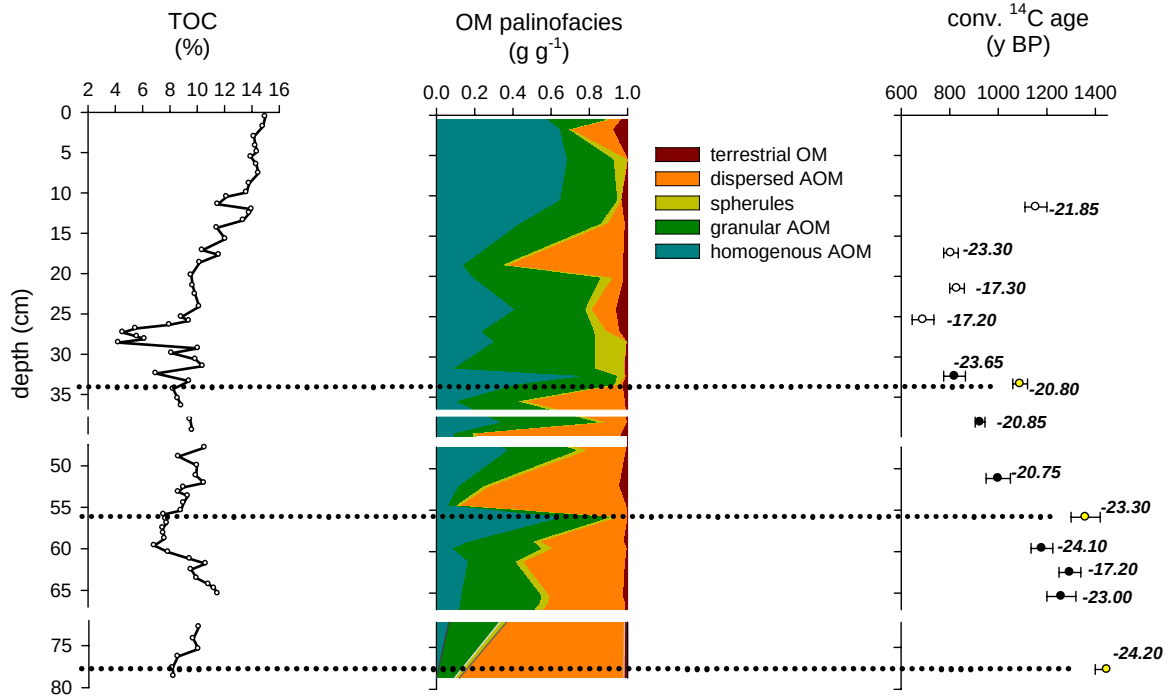
TOC
(%)
2 4 6 8 10 12 14 16
OM palinofacies
(g g-1)
0.0 0.2 0.4 0.6 0.8 1.0
terrestrial OM
dispersed AOM
spherules
granular AOM
homogenous AOM
conv. 14C age
(y BP)
600 800 1000 1200 1400
depth (cm)
0 5 10 15 20 25 30 35 50 55 60 65 75 80
-21.85
-23.30
-17.30
-17.20
-23.65
-20.80
-20.85
-20.75
-23.30
-24.10
-17.20
-23.00
-24.20

a

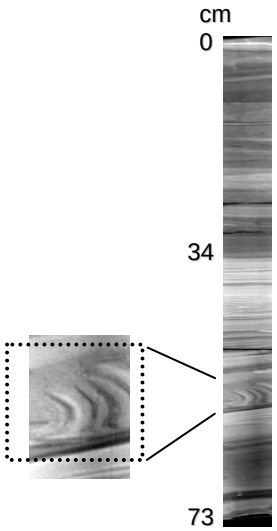
cm
0
34
73

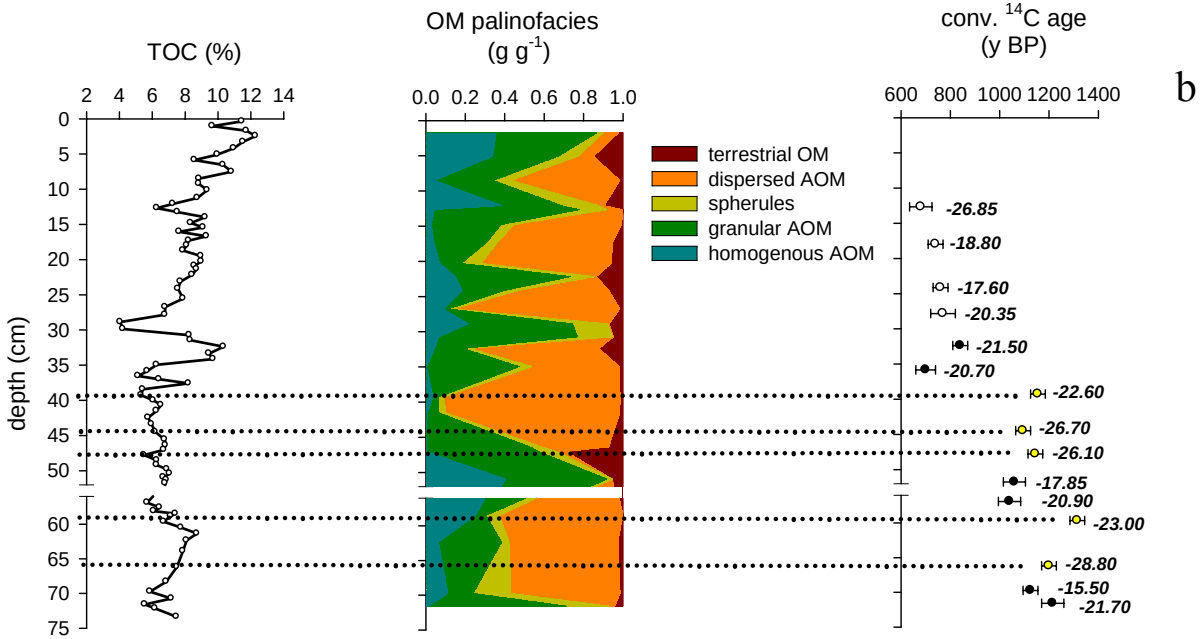
TOC (%)
2 4 6 8 10 12 14
OM palinofacies
(g g-1)
0.0 0.2 0.4 0.6 0.8 1.0
terrestrial OM
dispersed AOM
spherules
granular AOM
homogenous AOM
conv. 14C age
(y BP)
600 800 1000 1200 1400
depth (cm)
0 5 10 15 20 25 30 35 40 45 50 60 65 70 75
-26.85
-18.80
-17.60
-20.35
-21.50
-20.70
-22.60
-26.70
-26.10
-17.85
-20.90
-23.00
-28.80
-15.50
-21.70

b

SF3

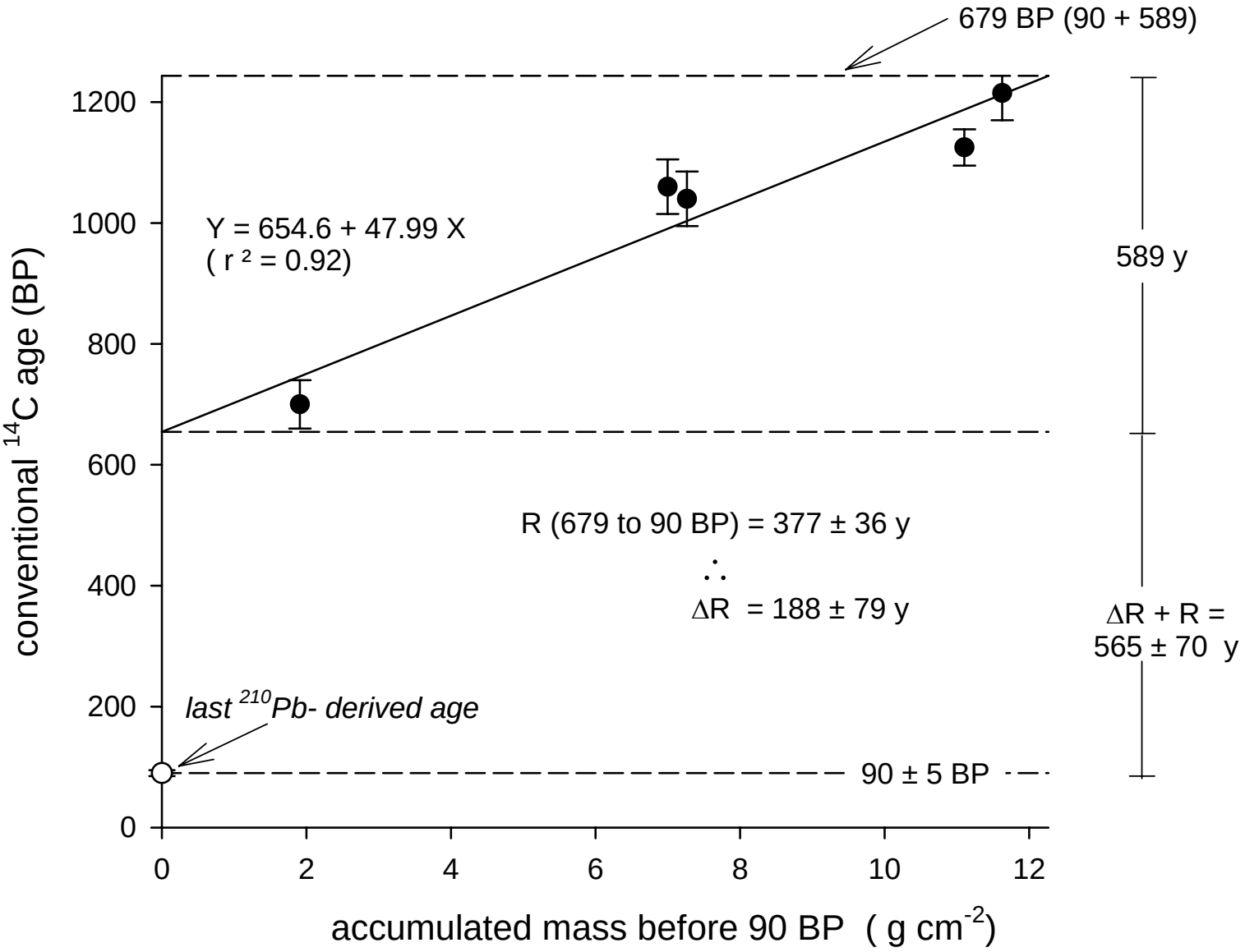
679 BP (90 + 589)
Y = 654.6 + 47.99 X
(r ² = 0.92)
589 y
R (679 to 90 BP) = 377 ± 36 y
∴
ΔR = 188 ± 79 y
ΔR + R =
565 ± 70 y
last 210Pb- derived age
90 ± 5 BP
conventional 14C age (BP)
accumulated mass before 90 BP (g cm-2)
0
200
400
600
800
1000
1200
0
2
4
6
8
10
12